IJRAR.ORG E-ISSN: 2348-1269, P-ISSN: 2349-5138

INTERNATIONAL JOURNAL OF RESEARCH AND ANALYTICAL REVIEWS (IJRAR) | IJRAR.ORG

An International Open Access, Peer-reviewed, Refereed Journal

TWIP Steel Advances: Increasing Corrosion Resistance in Automotive, Structures, and Electrical Applications

Nicky Kisku[1], Deepak Sau[2] , Twinkle Kisku[3]

Department of Metallurgical and Materials Engineering, Indian Institute of Technology, Kharagpur, 721302, India[1]

National Metallurgical Laboratory, Jamshedpur, 831007, India[2]

Department of Electrical Engineering, Odisha University of Technology and Research, Bhubaneswar, 751029, India[3]

Abstract

The present study focuses on the effect of alloying elements and microstructural modification on corrosion property of the investigated steel. An attempt has been taken to advance the corrosion resistance of twinning induced plasticity Fe-12Mn-0.6C-4Al-7Si-0.2Ti steel. The developed TWIP steel was undergone to hot forging followed by hot rolling. The impact of grain boundary engineering (GBE) on the six-month corrosion and rusting behavior of hot-rolled and forged specimens. Formation of twins after hot rolling treatment greatly improved the corrosion property as well as the mechanical property of the specimens. An association of random high angle grain boundaries (HAGBs) is observed for forged sample which detoriates both the above mentioned properties. Considerable segregation of major alloying elements like Mn and Si through the grain boundaries is evident in the forged specimen. On the other hand, the hot rolled sample shows significant restriction to atmospheric corrosion and elemental segregation in the grain boundary. This considerable corrosion resistance is due to the presence of more fraction of twin Σ3 CSLs (35%) which opposed the occurrence corrosion in the material. In addition to the corrosion property, the tensile property was also observed to be significantly improved (UTS= ~1600 MPa, % elongation11) in hot rolled specimen.

key words: Thermo-mechanical Process, Grain Boundary Modification, Twins, High Strength, High Corrosion Resistance

1. Introduction

The integration of advanced materials has long been at the forefront of innovation in engineering disciplines, offering solutions to a diverse array of challenges. Among these materials, Twinning Induced Plasticity (TWIP) steel has emerged as a remarkable contender, celebrated for its exceptional properties in strength, formability, and notably, corrosion resistance [1-5]. In this comprehensive study, we delve into the multifaceted TWIP steel and its profound impact on three distinct but interconnected engineering fields: automotive, structural, and electrical engineering. Through this exploration, we aim to unveil the pivotal role that TWIP steel plays in each of these domains, shedding light on the latest advancements and its enduring relevance in our ever-evolving technological landscape. Electrical steel also known as silicon steel, is a specialized type of steel that is designed for use in electrical devices and transformers [2]. It has specific properties that make it suitable for these applications. Iron is the primary component of electrical steel, making up the majority of its composition. Silicon is the most critical alloying element in electric steel [6]. It is added in varying percentages, typically ranging from 2% to 4.5%. The silicon content is what gives electrical steel its magnetic properties, including high electrical resistivity and low core loss, making it suitable for use in transformers and other electromagnetic devices. Carbon (C): Carbon content in electrical steel is kept very low, usually less than 0.005%. This low carbon content helps reduce hysteresis losses and improves magnetic properties. Other elements such as aluminum (Al) and Manganese (Mn), which can further enhance its magnetic properties and processing characteristics [6].

Grain boundary engineering (GBE) has been demonstrated to be a successful method for improving the performance and characteristics of polycrystalline materials [7-9]. The GBE entails changing the nature of the grain boundary and its distribution in order to increase the fraction of special boundaries in the microstructure using a thermo-mechanical processing schedule [1]. Special type of boundaries are those that have comparatively better properties as compared to the random high-angle grain boundaries (HAGBs) and are generally described in terms of the coincidence site lattice (CSL) model. It is generally assumed that low Σ ($\Sigma \leq 29$) CSL boundaries are 'special' even though there is no physical basis for this assumption [3]. According to recent findings, only a subset of low CSLs are unusual [2]. Given that, the GBE technique has been shown to be effective in improving the characteristics of several low-to-medium stacking fault energy materials [4]. This is primarily because this hot rolled specimen exhibits extensive multiple twinning during thermo-mechanical (GBE-type) processing, resulting in a higher fraction of'special' 3 boundaries visible on the low-index plane [4]. These higher order twin boundaries take part in the reconstruction of the obtainable grain boundary network that ultimately breaks the random HAGBs connectivity and prevents corrosion [5,7].

Although the GBE approach has been widely used in the past to reduce inter-granular corrosion of various low-to-medium stacking fault energy materials in aqueous corrosion medium, very little effort has been made to investigate the impact of GBE on high temperature atmospheric corrosion of twin induced high strength steel. [9-11]. Therefore, the reaction between the Fe-12Mn-0.6C-4Al-7Si-0.2Ti steel and air, primarily consisting of oxygen (O_2) at room temperature. Considering the contribution of all the elements in the high Si, high Mn TWIP steel was developed to study the corrosion resistivity. The developed TWIP steel was undergone to hot forging followed by hot rolling. The present study focuses on the cause of alloying elements and microstructural modification on corrosion property of the investigated steel.

2. Methods

Exposing TWIP (Twinning Induced Plasticity) steel to weather conditions for an extended period like 6 months is a controlled experiment that requires careful planning and monitoring. The Fe-12Mn-0.6C-4Al-7Si-0.2Ti steel used in the investigation was prepared through melting casting routes, forged (at 1373K) and quenched with water. The forged specimens were subjected to hot rolled with 20% reduction in thickness followed by water quenching. The hot rolling (1173 K) with 30% reduction. Hot rolling at 1173K followed by water quenching resulted in a GBE microstructure having high fraction of twins (Σ3 boundaries) and remarkable obstruction in random HAGBs connectivity. TWIP steel samples were obtained with the desired dimensions and surface finish. The sample surfaces were cleaned to remove any contaminants or impurities that could interfere with the corrosion process. Labeling was done on each sample to ensure proper identification throughout the exposure period. The TWIP steel samples were mounted in a way that simulates their intended use or orientation. Utilization of racks, frames, or supports to keep the samples stable and secure. Periodically inspecting the TWIP steel samples. A consistent inspection scheduling was established for 6 months to assess changes in the steel's condition. Record observations, noting any visible corrosion, changes in appearance, or degradation of the steel's surface. Detailed records were maintained of the exposure experiment, including sample identification, exposure conditions, inspection dates, and any relevant observations or measurements. After the 6-month exposure period, the TWIP steel samples were carefully remove from the exposure site. The condition of each sample was documented. Comparison of the properties of forged and hot rolled conditions exposed to weather conditions were done to study the corrosion behavior. Standard metallography processes were used to polish both the forged and hot rolled specimens. TSL OIM analysis software (version 7.2) was used to generate EBSD maps from processed samples with a scan area of 100X100 μm^2 and a step size of 0.5 mm. Brandon's criterion is used to categorize CSL borders [7] . Random HAGBs are those with a misorientation angle more than 15° that are not low (Σ29) CSL limits. SEM and combined EBSD/energy dispersive spectroscopy (EDS) were used to examine the cross sections of both specimens to determine the degree of hot corrosion attack on the specimens.

3. Results and discussion

3.1. Microstructural Analysis

Microstructural analysis of forged and hot rolled specimens of TWIP (Twinning Induced Plasticity) steel involves examining the internal structure of the material at a microscopic level to understand how the manufacturing thermo-mechanical processes of forging and hot rolling affect its corrosion properties. The forged specimen microstructure shows large equiaxed austenite with grain size ~89±3 μm (Fig 1(a)). The lower deformation temperature (i.e., 1173 K) during hot rolling reduced the overall grain size from 89± 4 μm after forging to 18± 3μm after hot rolling (Fig. 1(c)). The XRD plots in Figs. 1 (b) and (d) show the phase distribution for hot forged and hot rolled specimens, respectively. The amount of martensite increases dramatically from 3% in hot forged conditions to 24% in hot rolling conditions (Fig. 1(b,d)). The x-ray diffraction profiles in Fig. 1(b) demonstrate a fully austenitic structure (a = 3.60) for the hot forged specimen with pronounced austenite peaks at 2 = 44˚ and 50˚. XRD analysis does not reveal the presence of strain-induced martensite in this case. Here, the presence of strain-induced ε-martensite is not apparent from XRD profile (see Fig. 1(b)). The formation of strain-induced ε-martensite (a = 4.54, b = 4.54, c = 6.88 Å) and α'-martensite (a = 2.84 Å) in the austenite matrix is observed. However, some traces of strain-induced martensite are observed in hot rolled specimen (Fig. 1d)

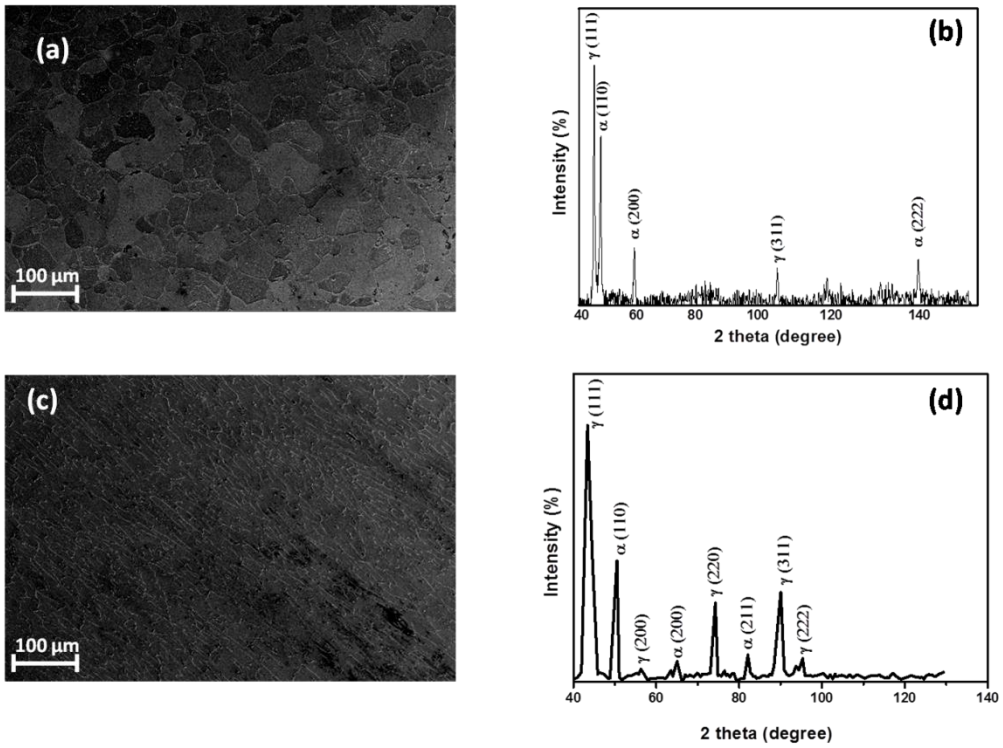

Figure 1: Optical micrograph illustrating (a) the microstructure of forged specimen (b) its corresponding XRD plot, (c) micrograph of hot rolled specimen, (d) XRD plot of hot rolled specimen

Reactions:-

Oxidation of Iron (Fe):

Iron in the steel alloy reacts with oxygen (O_2) from the air to form iron oxides. The most common iron oxide that forms is iron(III) oxide (Fe_2O_3), often referred to as rust.

The reaction can be represented as follows:

$4Fe + 3O_2 \rightarrow 2Fe_2O_3$

This initial oxidation process results in the formation of a reddish-brown rust layer on the surface of the steel.

Formation of Manganese Oxides:

At room temperature, manganese slowly oxidizes in the presence of oxygen from the air. The initial product is typically a mixture of manganese oxides, with manganese(II) oxide (MnO) being one of the prominent compounds formed.

The reaction can be represented as:

$2Mn + O_2 \rightarrow 2MnO$

At elevated temperatures or in the presence of more oxygen, manganese can further react to form higher oxides. Manganese dioxide (MnO_2), which is a common natural mineral called pyrolusite, is one of the higher oxides formed [12].

The reaction leading to manganese dioxide formation is:

$2MnO + O_2 \rightarrow 2MnO_2$

Formation of Aluminum Oxide (Al_2O_3):

Aluminum (Al) in the alloy reacts with oxygen to form aluminum oxide (Al_2O_3). This aluminum oxide layer provides some protection against further corrosion by acting as a barrier [13].

The reaction can be represented as:

$4Al + 3O_2 \rightarrow 2Al_2O_3$

Silicon Oxide Formation (SiO_2):

Silicon (Si) in the alloy can contribute to the formation of silicon oxide (SiO_2) on the surface, further enhancing the protective oxide layer. Silicon (Si) reacts with air, specifically with oxygen (O_2), to form silicon dioxide (SiO_2), which is commonly known as silica or silicon oxide. This reaction is relatively slow and requires elevated temperatures to proceed at a noticeable rate [11-15]. Here's the reaction that occurs when silicon reacts with oxygen in the air:

$2Si + O_2 \rightarrow 2SiO_2$

In this reaction, two silicon atoms (2Si) combine with one molecule of oxygen (O_2) to produce two molecules of silicon dioxide ($2SiO_2$). Silicon dioxide is a compound that consists of silicon and oxygen atoms arranged in a crystal lattice structure [6]. It is a hard, amorphous or crystalline material with various applications, including as a component of glass, ceramics, and semiconductor materials [6].

Role of Titanium (Ti):

Titanium (Ti) can form titanium oxides or nitrides, depending on the specific conditions. These compounds can also contribute to the protective barrier on the steel surface.

The combination of these reactions results in the formation of protective oxide layers, primarily composed of iron oxides (rust), aluminum oxide (Al_2O_3), and silicon oxide (SiO_2). These oxide layers serve as a passive barrier, reducing the rate of further corrosion by limiting the exposure of the underlying metal to the environment [8]. The effectiveness of this protection depends on various factors, including the composition of the alloy, the presence of impurities, and the environmental conditions (humidity, temperature, pollutants). In many cases, these protective oxide layers can slow down the corrosion rate of the steel alloy significantly, but over very long periods, corrosion may still occur [7].

3.2. *Microstructural observation after corrosion*

Figure 2 shows the SEM microstructure of the hot corrosion tested specimens. When Figs. 2a-c (forged specimen) and 2b-d (hot rolled specimen) are compared, it is clear that the corrosion attack has penetrated deeper in the forged specimen, whereas percolation has been stopped in the GBE modified hot rolled specimen. The observed depth of penetration due to intergranular corrosion of forged specimen across the whole cross section is ~3 mm (as shown in Fig 2a). However, the depth of penetration in a hot rolled specimen was only 300 µm (Fig. 2b). Atmospheric corrosion is a very complex phenomena that involves numerous reactions occurring at the same time. Figure 2 (a,b) reveals the presence of rust layers on the surface of the steel. Rust appears as a reddish-brown, flaky or powdery material. The thickness and distribution of rust on the steel's surface can indicate the degree of corrosion of the forged specimen. Corrosion can affect the grain structure of the steel. Microstructural analysis can help identify changes in grain size or orientation that may have occurred due to corrosion-induced damage [5]. In case of hot rolled specimen (Fig.2b), it is observed that it is corrosion resistive as compared to the forged specimen, due to the presence of twins (Σ3) which restricts the corrosion behavior of the hot rolled specimen (Fig. 2d). In some cases, twin boundaries (Fig.2d) can enhance the corrosion resistance of a material. Sigma three twin boundaries can act as barriers to the movement of corrosive species, such as ions or water molecules, preventing them from penetrating deeper into the material [4-7].

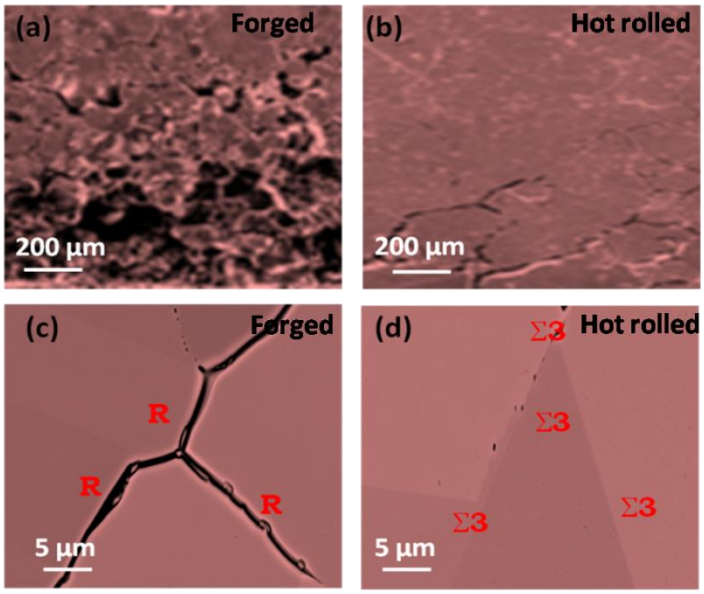

Figure 2. SEM images of cross-section showing the intergranular damage due to hot corrosion in (a) forged (b) hot rolled specimens. and (c) random HAGBs in forged, (d) Σ3 boundaries in rolled specimen

3.3 Effect of microstructural modification on corrosion

The grain boundary EBSD map reveals large grains (in forged condition) undergoes grain refinement after hot rolling (3a-b). The average grain size (measured using the linear intercept method) in the forged condition was 89±2 µm (twin borders were used as grain boundaries). Because of the nucleation of a large number of twin boundaries in the microstructure, the grain size after hot rolling was reduced to 18 ±1.2 µm. The 3 fraction was found to be 5± 0.5% in the forged specimen and 35± 2% in the rolled specimen. Following thermomechanical processing, the fraction of 3 has been greatly increased. The improved fraction of Σ3 is an important condition to achieve the optimized rolled microstructure [8]. The research reveals that the fraction of connected Σ3-CSL boundaries has grown significantly after thermomechanical processing (3c-d). The connectivity of Σ3-CSL boundary would indicate a GBE microstructure [7,8]. Twin boundaries can serve as partial grain boundaries,

which are generally less susceptible to corrosion compared to high-angle grain boundaries. This reduced susceptibility to grain boundary corrosion can be advantageous [8]. Figure 3(e-f) illustrates the distribution of random high angle grain boundaries and CSL boundaries. It is observed that forged specimen contains higher fraction of random HAGBs (Fig. 3e) where as hot rolled specimen comprises of higher fraction of Σ3 CSL-boundaries (Fig. 3f). The random HAGBs are the preferential sites for percolations, where as the origination of special Σ3 CSL-boundaries restricts the percolation [4-9]. Hence, the higher fraction of Σ3 CSL-boundaries in hot rolled specimen offers better corrosion resistive property.

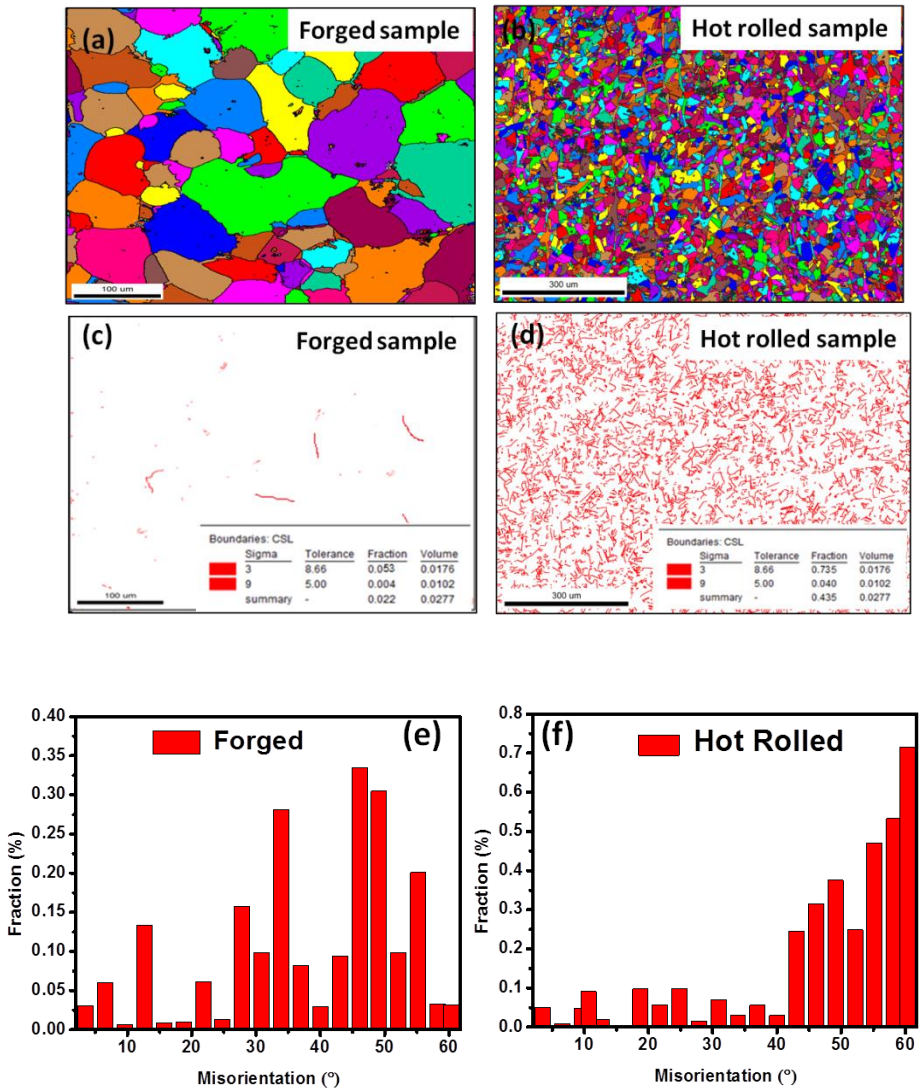

Figure 3: EBSD grain orientation spread map showing volume fraction of recrystallized grain of (a) hot forged and (b) hot rolled specimen. Twin fraction map after (c) forging, (d) hot rolling. Distribution of LAGBs and HAGBs in (e) forged (f) hot rolled specimen

3.4 Effect of alloying elements

Figure 4a,b shows the distribution of major alloying elements Mn and Si for forged and hot rolled specimens. The alloying elements manganese (Mn) and silicon (Si) can have both beneficial and detrimental effects on segregation during corrosion, depending on the specific conditions and alloy compositions. In forged condition (Fig. 4a) The effect of manganese on segregation can be complex and depends on the overall alloy composition. In present study, excessive manganese content contributes to microstructural changes that can increase susceptibility to pitting or crevice corrosion. The segregation of Mn in the grain boundary is evident in Fig.4a which is expected to decorate the corrosion as well as mechanical properties of the investigated steel. Whereas in hot rolled condition (Fig.5b) the addition of manganese to steel can help reduce segregation during corrosion. Manganese can form oxide compounds that have a similar solubility in the steel matrix, which minimizes the tendency for Mn to segregate at grain boundaries or other microstructural features [10]. Manganese can contribute to the formation of protective oxide layers on the surface of the material, which can reduce corrosion rates. These protective layers can help prevent preferential corrosion along grain boundaries or other segregated regions [13]. The silicon forms non-protective phases or compounds that can exacerbate corrosion in forged condition (Fig.4c). The behavior of silicon depends on its concentration and the specific environmental conditions. In hot rolled specimen silicon has a positive impact on corrosion resistance by reducing the susceptibility to grain boundary corrosion (Fig.4d). Silicon can form silicon oxide (SiO_2) at grain boundaries, which acts as a protective barrier against certain types of corrosion [11]. The presence of silicon is expected to enhance the passivity of the material, reducing the rate of corrosion in hot rolled condition. This is particularly beneficial in environments where passivation is essential for corrosion resistance.

It is noteworthy to note that hot corrosion has caused Mn and Si segregation at random HAGBs in forged specimens (Fig. 4a,c). In contrast, the hot rolled specimen with three boundaries shows no preferential amplification of any alloying element in the grain boundaries, indicating that these borders are resistant to heat corrosion (Fig. 4b,d). The Σ3 boundaries along the low index (111) plane have very low interfacial energy, lowering the risk of intergranular corrosion [9-15].

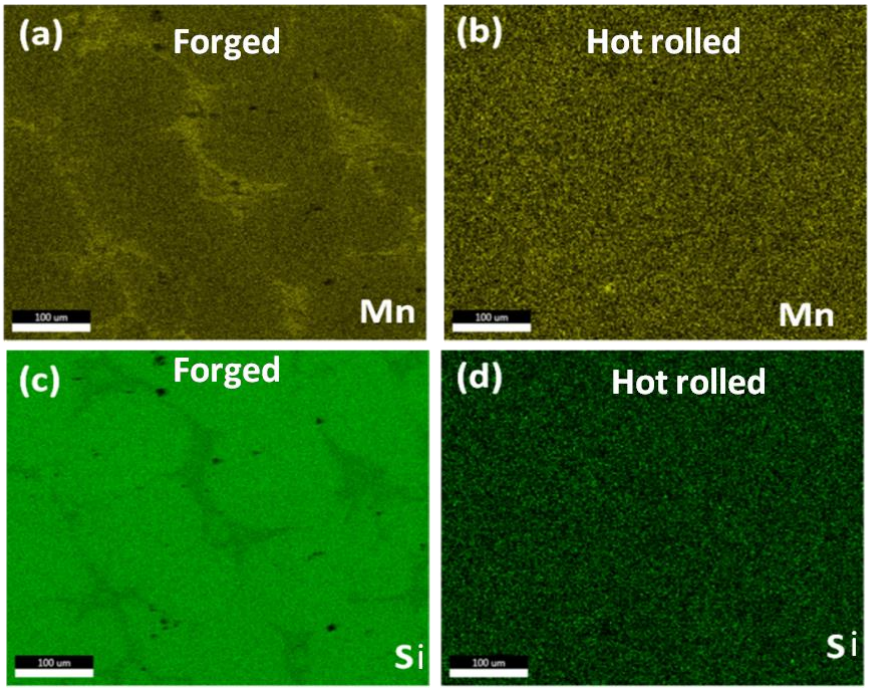

Figure 4. Segregation of alloying elements during corrosion in forged specimen (Fig. 4a and c), and in GBE modified hot rolled specimen (Fig. 4b and d)

3.5 Enhancement in Mechanical Properties due to presence of twins:

Materials with well-defined twin boundaries may exhibit improved mechanical properties, such as higher strength and ductility. These properties can indirectly contribute to corrosion resistance by reducing the likelihood of mechanical damage that can lead to corrosion initiation [11]. Figure 5(a) shows typical engineering stress-strain data for forged and hot rolled specimens. The hot rolled specimens evidently show enhanced tensile strength (UTS~1600±10 MPa) in comparision to forged one (UTS~ 800±13 MPa) with no substantial change in elongation (~ 11%) for hot rolled specimen and ~12% elongtion in forged condition. Twinning typically occurs as a mechanism for plastic deformation in materials. When an external force is applied to the material, dislocations are generated within the crystal lattice. Twinning causes a change in the atomic arrangement and results in localized strain within the crystal structure. This localized strain can lead to strain hardening, which is an increase in the material's strength due to the plastic deformation [19]. Twin boundaries act as barriers to dislocation motion (as seen in Fig. 5b). When dislocations encounter a twin boundary, they can be impeded or even absorbed by the boundary. This increases the resistance of the material to plastic deformation and contributes to its overall strength. Hot rolled specimen undergone twinning exhibits an improved balance between strength and ductility [20]. While becomes stronger due to strain hardening and the presence of twin boundaries, they may maintain reasonable levels of ductility compared to materials that rely solely on grain boundary strengthening or solid solution strengthening. To understand the nature of twins, twin-dislocation interaction, TEM analyses were carried out for hot rolled specimens. Figure 5(b) demonstrates the presence of twins and their interaction with the dislocation on the austenitic matrix in 1173K-HR 30% red. specimen, as confirmed by its corresponding SADP (Fig. 5(c)). The presence of dislocation is also evident, where the twin boundaries, are hindering the movement of dislocations [5,12, 13]. The generation of deformed twins and are controlled by the SFE of the material [22-25]. Due to the occurence of the twins formation of crack gets restricted. Therefore, from the above studies it is evident that the formation of twins prevent the specimen from getting corroded and increseas the longitivity of the materials exposed in environment.

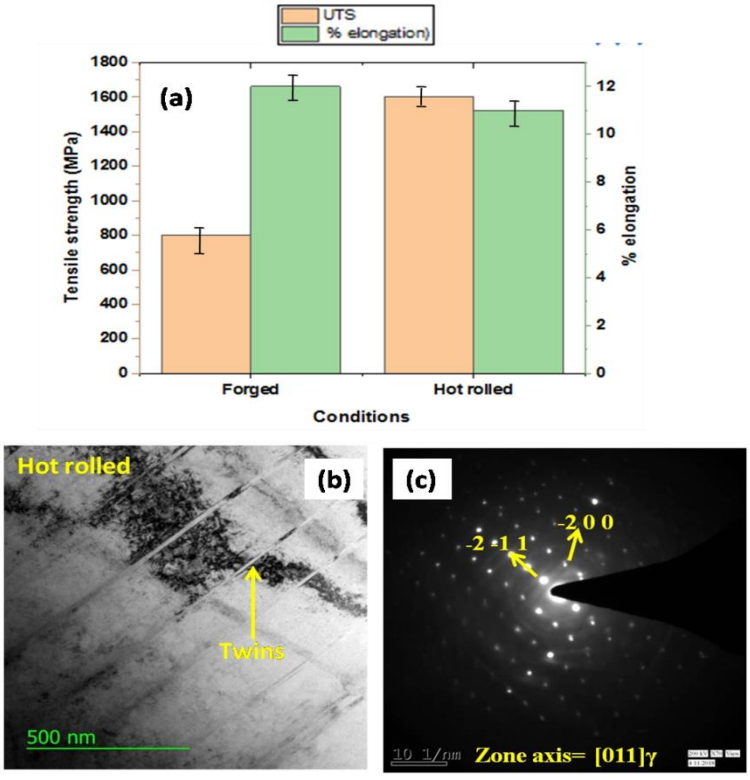

Figure 5: The TEM micrograph revealing the twins in the (a) hot rolled specimens (b) SADP of hot rolled specimen

4. Conclusions

By exposing both the forged and GBE hot rolled specimens in open air weather conditions, the effect of grain boundary engineering on hot corrosion behavior of Fe-12Mn-0.6C-4Al-7Si-0.2Ti steel was established. Due to oxide depletion in the random HAGBs, the forged specimen has low corrosion resistance. By adopting thermo-mechanical processing (hot rolled at 1173K) significant occurance of twins have been observed which prevented the corrosion behaviour and increased the tensile strength of the investigated steel. Due to the presence of CSL-Σ3 boundaries the hot rolled specimen is restricted to atmospheric corrosion. The higher fraction of CSL-Σ3 boundaries (twins) in the GBE-hot rolled specimen restricts the random boundaries network which arrest the percolation.

"On behalf of all authors, the corresponding author states that there is no conflict of interest."

References

1. P. Podany, T. Gregor, High Manganese TWIP Steel with Increased Corrosion Resistance, Metals (2022), 12(10), 1765
2. A. Kozłowska, P. Stawarczyk, A. Grajcar & L. Samek, Microstructure evolution and strain hardening behavior of thermomechanically processed low-C high-manganese steels: an effect of deformation temperature, Archives of Civil and Mechanical Engineering, 184 (2023). 1-23.
3. R. Jones, V. Randle, Sensitization behaviour of grain boundary engineered austenitic stainless steel, Mater. Sci. Eng. A 527 (2010) 4275–4280.
4. 2. Y. Takehara, H. Fujiwara, H. Miyamoto, Special to general transition of intergranular corrosion in Σ3{1 1 1} grain boundary with gradually changed misorientation, Corros. Sci. 77 (2013) 171–175.
5. A. Stratulat, J.A. Duff, T. James Marrow, Grain boundary structure and intergranular stress corrosion crack initiation in high temperature water of athermally sensitized austenitic stainless steel, observed in situ, Corros. Sci. 85(2014) 428–435.
6. V. Randle, Grain boundary engineering: an overview after 25 years, Mater. Sci. Technol. 26 (2010) 253–261.
7. B. Sunil Kumar, B.S. Prasad, V. Kain, J. Reddy, Methods for making alloy 600resistant to sensitization and intergranular corrosion, Corros. Sci. 70 (2013), 55–61.
8. M.H. Habibi, L. Wang, J. Liang, S.M. Guo, An investigation on hot corrosion behavior of YSZ-Ta_2O in Na_2SO_4+ V2O5salt at 1100◦C, Corros. Sci. 75 (2013), 409–414.
9. D.G. Brandon, The structure of high-angle grain boundaries, Acta Metall. 14(1966) 1479–1484.
10. N. Eliaz, G. Shemesh, R.M. Latanison, Hot corrosion in gas turbine components, Eng. Fail. Anal. 9 (2002) 31–43.
11. C.A. Schuh, M. Kumar, W.E. King, Analysis of grain boundary networks and their evolution during grain boundary engineering, Acta Mater. 51 (2003) 687–700.
12. J. Z. Albertsen and R. H. Mathiesen, Metallurgical investigation of metal dusting corrosion in plant-exposed nickel-based alloy 602CA, Corrosion Engineering, Science and Technology. 40 (2005) 239-241.
13. M. Li, X. Sun, W. Hu, H. Guan, S. Chen, Hot corrosion of a single crystal Ni-base superalloy by Na-Salts at 900◦C, Oxid. Met. 65 (2006) 137–150.
14. S. Zhao, X. Xie, G.D. Smith, The oxidation behavior of the new nickel-based superalloy Inconel 740 with and without Na_2SO_4deposit, Surf. Coat. Tech. 185 (2004) 178–183.

15. Z. Tang, Xia Dong, X. Mei, The effect of warm laser shock peening on the thermal stabilityof compressive residual stress and the hot corrosion resistance of Ni-based single-crystal superalloy, Optics & Laser Technology 146, (2022), 107556

16. D. Blöcher, G. Frommeyer, & R. Hehemann, Influence of carbon on stacking fault energy and plastic deformation in twinning-induced plasticity steels. Acta Materialia, 50(5), (2002) 1025-1043.

17. Ghassemi-Armaki, H., & Svensson, J. E. Stress corrosion cracking of austenitic high manganese twinning-induced plasticity steel in contact with chloride-containing solutions. Corrosion Science, 81, (2014), 70-80.

18. M. Koyama, Corrosion behavior of high manganese austenitic steel with partial twinning. Corrosion Science, 147, (2019), 45-55.

19. T. Mukai, Influence of deformation twins on the corrosion behavior of Fe-30Mn-3Al-3Si TWIP steel. Corrosion Science, 111, . (2016) 166-174.

20. C.Ouyang Corrosion behavior of Fe-Mn-C twinning-induced plasticity steel in simulated marine environments. Corrosion Science, 168, (2020), 108569.

21. Y. Pei, Investigation of corrosion behavior in twinning-induced plasticity steel under different atmospheric environments. Materials and Corrosion, 72(2), (2021), 214-224.

22. A., Saeed -Akbari, & J. E. Svensson, The role of deformation twinning on the corrosion behavior of high manganese twinning-induced plasticity steel in chloride solutions. Corrosion Science 90, (2015), 484-496.

23. B. B. Sahoo, Effect of pre-strain and microstructure on the corrosion behavior of Fe-30Mn-3Al-3Si twinning-induced plasticity steel. Journal of Materials Research and Technology, 9(6), (2020), 15339-15351.

24. N. Schlegel, Corrosion behavior of Fe-Mn-Al-Si twinning-induced plasticity steel in aqueous environments. Corrosion Science, 117(2017), 157-166.

25. Sedighi, M., et al. (2018). Investigation of the corrosion behavior of twinning-induced plasticity steel in chloride-containing environments. Journal of Materials Engineering and Performance, 27(9), 4851-4862.